Author(s): Airaksinen, Tuomas; Toivanen, Jari

Title: Quadratic least-squares formulation for a local active noise control with stochastic domain and noise source

Year: 2012

Version:

Please cite the original version:

Airaksinen, T., & Toivanen, J. (2012). Quadratic least-squares formulation for a local active noise control with stochastic domain and noise source. In J. Eberhardsteiner, H. Böhm, & F. Rammerstorfer (Eds.), Proceedings of the 6th European Congress on Computational Methods in Applied Sciences and Engineering (ECCOMAS 2012). Wien: Vienna University of Technology.

European Congress on Computational Methods
in Applied Sciences and Engineering (ECCOMAS 2012)
J. Eberhardsteiner et.al. (eds.)
Vienna, Austria, September 10-14, 2012

QUADRATIC LEAST-SQUARES FORMULATION FOR A LOCAL ACTIVE NOISE CONTROL WITH STOCHASTIC DOMAIN AND NOISE SOURCE

Tuomas Airaksinen[1], **Jari Toivanen**[2]

[1]Department of Mathematical Information Technology
University of Jyväskylä
P.O. Box 35 (Agora), FI-40014 University of Jyväskylä, Finland
email: tuomas.a.airaksinen@jyu.fi

[2] Institute for Computational and Mathematical Engineering
Durand Building, Stanford University, Stanford, CA 94305, USA
email: toivanen@stanford.edu

Keywords: local sound control, stochastic domain, helmholtz equation, finite element method, passenger car, quadratic optimization

Abstract.

A local active noise control method that uses stochastic numerical acoustical modeling is introduced. The frequency domain acoustical simulations are performed by a sequence solutions to Helmholtz equations approximated by FEM. The proposed ANC method maps microphone measurements linearly to the output signals of antinoise actuators. The matrix defining the linear mapping is optimized for each frequency to minimize expected value of the noise. The paper concentrates on defining the quadratic least-squares optimization problem for the minimization of the sound pressure field in the silent region. The formulation leads to a robust and accurate noise control in stochastic domains that has a stochastic noise source. The method is demonstrated numerically by an experiment in a car cabin, and significant noise reduction is demonstrated at lower frequencies.

1 INTRODUCTION

In urban environment, noise is considered generally as an annoyance and thus it is necessary to reduce it in various environments. Engineering vehicles and passenger cars are examples of domains, where active noise control (ANC) methods could be efficiently applied. ANC [8] especially good at reducing low frequency noise. In ANC, noise is cancelled by an antisound that has the same amplitude but opposite phase, causing destructive interference to the sound field. Often it is desired to be able to reduce noise in certain part of the acoustical space, and there local noise control methods could be used to obtain satisfactory results.

A passenger car is a typical example of an application in which active noise control could be used. There, noise is desired to be silenced nearby the head locations of driver and passengers. Many recent publications on ANC focus on passenger car or related enclosures, and the most sophisticated methods involve numerical simulation and optimization [7, 12, 10, 11]. Particularly local noise control methods have been studied in [6, 5, 14].

Many practical applications involve stochasticity naturally in their acoustical domain, i.e. there are random, time-dependent changes in the domain that manipulate the sound field significantly. In passenger car, for example, engine parts and passengers move. Stochastic domains can be used conveniently to model such geometry changes. In a stochastic domain, the expected value of the noise is computed as a numerical integral of product of the noise and the probability distribution over the probability space. By this way, it is possible to use a solution methods for non-stochastic problems, like the method introduced in [2, 4], without modifications.

The method that we consider in this paper, determines the optimal performance for local noise control in a stochastic cavity domain. The anti-noise actuator signals are optimized such that the numerically computed expected value of the noise is minimized. This novel technique was first introduced in [3], and in [1] it was used to further develop a method to find optimal anti-noise actuator locations.

The ANC evaluation method in [3, 1] could be used to investigate the possibilities of proposed active noise control techniques, but it could not be implemented in a real ANC system due its limitations. The method lacked the stochasticity of the noise source, relying on a rough deterministic model of the noise source. The method also assumed constant phase and amplitude, which kept the method from being used in real applications where the phase and amplitude are not precisely known. We will tackle these limitations in this paper by a stochastic noise source and an approach to determine the optimal anti-noise actuators signals by using real-time data from a number of measurement sensors.

The local noise control approach in this paper is remarkably novel, and, to author's best knowledge, no other similar approach are presented in the literature. While there are many papers on local ANC methods that utilize numerical simulations to examine their method's abilities, or optimize microphone or anti-noise actuator locations, they are most commonly based on linear identification and control techniques that can be implemented purely by using digital signal processing circuitry. On the other hand, the approach on this paper is based on numerical acoustical simulations; sensor measurements are used only to obtain accurate phase and amplitude information to the model. The method has a major advantage over traditional methods: by acoustical simulations, it uses much more information of the sound field than could be obtained by measurement sensors.

This article is organized as follows. In Section 2, we present briefly the mathematical model of sound propagation (Helmholtz equation and associated boundary conditions), and a method to solve it numerically. In Section 3, the local noise control in a stochastic domain is formulated

as a quadratic optimization problem. In Section 4, the numerical method is demonstrated by a three-dimensional car cabin problem. In Section 5, conclusions are given.

2 ACOUSTIC MODEL

In this study, the sound propagation is modeled by the Helmholtz equation

$$-\boldsymbol{\nabla}\cdot\boldsymbol{\nabla}p-\frac{\omega^2}{c^2}p=0 \quad \text{in}\,\Omega, \tag{1}$$

where c is the speed of sound, ω is the angular frequency and p is the complex sound pressure defining the amplitude and phase of the sound pressure. The sound pressure at time t is obtained by $\mathfrak{Re}\left(e^{-i\omega t}p\right)$, where $i=\sqrt{-1}$.

A partially absorbing wall material is described by the impedance boundary conditions

$$\begin{aligned}\frac{\partial p}{\partial \mathbf{n}}&=\frac{i\eta\omega}{c}p+f \quad && \text{on } S\\ \frac{\partial p}{\partial \mathbf{n}}&=\frac{i\eta\omega}{c}p && \text{on } \partial\Omega\setminus S,\end{aligned} \tag{2}$$

where η is the absorption coefficient of the surface material and f is the source term. Values 0 and 1 for η approximate sound hard material (Neumann boundary condition) and perfectly absorbing material (low order absorbing boundary condition), correspondingly.

The partial differential equation (PDE) (1) is approximated by finite element method (FEM) [13]. FEM discretization transforms (1) into a matrix equation $\mathbf{Ax}=\mathbf{b}$, where $\mathbf{A}$ is generally symmetric, large, and sparse matrix. Since the size and structure of $\mathbf{A}$ does not allow direct solution methods, it is necessary to use iterative solution methods like GMRES. Solving the system with a reasonable number of iterations is, however, challenging, as the matrix $\mathbf{A}$ is badly conditioned. In the numerical example in Section 4, the solutions are computed after the systems are preconditioned by a damped Helmholtz preconditioner [2, 4].

3 THE QUADRATIC NOISE CONTROL FORMULATION

3.1 Quadratic program (QP) formulation

We consider acoustic model in an enclosed stochastic domain, denoted by $\Omega(\mathbf{r})$, with stochastic variable $\mathbf{r}$ complying probability distribution $F_{\mathbf{r}}(\mathbf{r})$. The sound pressure $p\left(\mathbf{x},\mathbf{r},\mathbf{s},\boldsymbol{\gamma}\right)$ is due to stochastic noise source and n_a anti-noise actuators as follows:

$$p(\mathbf{x},\mathbf{r},\mathbf{s},\boldsymbol{\gamma}) \;=\; p_0(\mathbf{x},\mathbf{r},\mathbf{s})+\boldsymbol{\gamma}^T\mathbf{p}\left(\mathbf{x},\mathbf{r}\right), \tag{3}$$

where $p_0(\mathbf{x},\mathbf{r},\mathbf{s})$ is the sound pressure due to the stochastic noise source, with stochastic variable $\mathbf{s}$ complying probability distribution $F_{\mathbf{s}}(\mathbf{s})$;

$$\mathbf{p}\left(\mathbf{x},\mathbf{r}\right) \;=\; \left(p_1\left(\mathbf{x},\mathbf{r}\right),p_2\left(\mathbf{x},\mathbf{r}\right),\cdots,p_{n_a}\left(\mathbf{x},\mathbf{r}\right)\right)^T \tag{4}$$

is a vector of sound pressures due to n_a anti-noise actuators and $\boldsymbol{\gamma}=\left(\gamma_1,\ldots,\gamma_{n_a}\right)^T$ is the vector of complex coefficients γ_i determining the amplitudes and phases for each anti-noise source.

We will formulate the noise control problem such that the anti-noise actuator amplitudes γ_i are mapped from n_m measurement points contained in vector $\mathbf{m}=\left(m_1,\ldots,m_{n_m}\right)^T$ by a linear map that is defined by a $n_a\times n_m$ complex matrix $\mathbf{C}$:

$$\boldsymbol{\gamma} \;=\; \mathbf{Cm}. \tag{5}$$

The Eq. (3) now reads:

$$p(\mathbf{x},\mathbf{r},\mathbf{s},\mathbf{C}) \;=\; p_0(\mathbf{x},\mathbf{r},\mathbf{s}) + \mathbf{m}^T\mathbf{C}^T\mathbf{p}\left(\mathbf{x},\mathbf{r}\right). \tag{6}$$

The noise source, anti-noise actuators and measurement points are located on $\partial\Omega$. The elements of the matrix $\mathbf{C}$ are optimized to minimize the noise in a silent subdomain denoted by $V_C(\mathbf{r}) \subset \Omega(\mathbf{r})$. We will use a noise functional to measure the noise in silent region, defined by integral of square norm of the pressure over the silent region:

$$N(\mathbf{r},\mathbf{s},\mathbf{C}) = \int\limits_{V_C(\mathbf{r})} \left|p(\mathbf{x},\mathbf{r},\mathbf{s},\mathbf{C})\right|^2 \, d\mathbf{x}. \tag{7}$$

The relevant quantity with respect to optimization is the expected value of the noise functional (7), which is written as

$$E\left(N\left(\mathbf{r},\mathbf{s},\mathbf{C}\right)\right) = \int\limits_{\mathbf{r}}\int\limits_{\mathbf{s}} N\left(\mathbf{r},\mathbf{s},\mathbf{C}\right)\, F_{\mathbf{s}}\left(\mathbf{s}\right)\, d\mathbf{s}\, F_{\mathbf{r}}\left(\mathbf{r}\right)\, d\mathbf{r}. \tag{8}$$

If we approximate integrals in (8) by a numerical quadrature, we get an objective function

$$J(\mathbf{C}) = \sum_j w_j^{\mathbf{r}} \left[\sum_k w_k^{\mathbf{s}} N\left(\mathbf{r}_j,\mathbf{s}_k,\mathbf{C}\right) F_{\mathbf{s}}\left(\mathbf{s}_k\right)\right] F_{\mathbf{r}}\left(\mathbf{r}_j\right), \tag{9}$$

where $\mathbf{r}_j$ and $\mathbf{s}_j$ are the quadrature points, and $w_j^{\mathbf{r}}$ and $w_j^{\mathbf{s}}$ are weights for $\mathbf{r}$ and $\mathbf{s}$, correspondingly. An intermediate optimization problem now reads

$$\min_{\mathbf{C}} J(\mathbf{C}). \tag{10}$$

In order to obtain a convenient quadratic matrix formulation, we will next expand the integrand of (7):

$$\begin{aligned}
\left|p\left(\mathbf{x},\mathbf{r},\mathbf{s}\right)\right|^2 &= \left(p_0 + \mathbf{m}^T\mathbf{C}^T\mathbf{p}\right)\overline{\left(p_0 + \mathbf{m}^T\mathbf{C}^T\mathbf{p}\right)} \\
&= \left(p_0 + \mathbf{m}^T\mathbf{C}^T\mathbf{p}\right)\overline{\left(p_0 + \mathbf{p}^T\mathbf{C}\mathbf{m}\right)} \\
&= p_0\bar{p}_0 + \mathbf{m}^T\mathbf{C}^T\mathbf{p}\bar{p}_0 + \mathbf{m}^H\mathbf{C}^H\bar{\mathbf{p}}p_0 + \mathbf{m}^T\mathbf{C}^T\mathbf{p}\mathbf{p}^H\bar{\mathbf{C}}\bar{\mathbf{m}} \\
&= p_0\bar{p}_0 + \left(\mathbf{C}\mathbf{m}\right)^T\mathbf{p}\bar{p}_0 + \left(\bar{\mathbf{C}}\bar{\mathbf{m}}\right)^T\bar{\mathbf{p}}p_0 + \left(\mathbf{C}\mathbf{m}\right)^T\mathbf{p}\mathbf{p}^H\bar{\mathbf{C}}\bar{\mathbf{m}},
\end{aligned} \tag{11}$$

where overline symbol $^-$ denote element-wise complex conjugate.

Let us now denote ith column vector of matrix $\mathbf{C}$:n as $\mathbf{C}_i$, i.e. $\mathbf{C} = (\mathbf{C}_1, \mathbf{C}_2 \cdots \mathbf{C}_{n_m})$. Let us remember in the following, that $\mathbf{C}\mathbf{m} = \sum_{i=1}^{n_m} \mathbf{C}_i m_i$. Now we can further write

$$\begin{aligned}
\left|p\left(\mathbf{x},\mathbf{r},\mathbf{s}\right)\right|^2 &= p_0\bar{p}_0 + \left(\sum_{i=1}^{n_m}\mathbf{C}_i^T m_i\right)\mathbf{p}\bar{p}_0 + \left(\sum_{i=1}^{n_m}\bar{\mathbf{C}}_i^T\bar{m}_i\right)\bar{\mathbf{p}}p_0 \\
&\quad + \left(\sum_{i=1}^{n_m}\mathbf{C}_i^T m_i\mathbf{p}\right)\left(\sum_{j=1}^{n_m}\mathbf{p}^H\bar{\mathbf{C}}_j\bar{m}_j\right) \\
&= p_0\bar{p}_0 + \sum_{i=1}^{n_m}\left(\left(\mathbf{C}_i^T m_i\right)\mathbf{p}\bar{p}_0 + \left(\bar{\mathbf{C}}_i^T\bar{m}_i\right)\bar{\mathbf{p}}p_0\right) \\
&\quad + \sum_{i=1}^{n_m}\sum_{j=1}^{n_m}\mathbf{C}_i^T m_i\bar{m}_j\mathbf{p}\mathbf{p}^H\bar{\mathbf{C}}_j.
\end{aligned} \tag{12}$$

Now we can define the following notations: $\hat{a} = p_0\bar{p}_0$, $\hat{\mathbf{b}}_i = \bar{m}_i\bar{\mathbf{p}}p_0$ and $\hat{\mathbf{A}}_{ij} = m_i\bar{m}_j\mathbf{p}\mathbf{p}^H$, where superscript ^{H} denotes the Hermitian conjugate. It is easily seen that $\hat{\mathbf{A}}_{ij} = \hat{\mathbf{A}}_{ji}^H$:

$$\hat{\mathbf{A}}_{ji}^H = \bar{m}_j m_i \bar{\mathbf{p}}\mathbf{p}^T = m_i\bar{m}_j\mathbf{p}\mathbf{p}^H = \hat{\mathbf{A}}_{ij}. \tag{13}$$

We want to present the objective function (9) in a quadratic matrix form, and thus we will introduce the following notations:

$$\begin{aligned}
\mathbf{A}_{ij} &= \sum_j w_j^{\mathbf{r}} F_{\mathbf{r}}(\mathbf{r}_j) \sum_k w_k^{\mathbf{s}} F_{\mathbf{s}}(\mathbf{s}_k) \int_{\Xi(\mathbf{r})} \hat{\mathbf{A}}_{ij}\, d\mathbf{x} \\
\mathbf{b}_i &= \sum_j w_j^{\mathbf{r}} F_{\mathbf{r}}(\mathbf{r}_j) \sum_k w_k^{\mathbf{s}} F_{\mathbf{s}}(\mathbf{s}_k) \int_{\Xi(\mathbf{r})} \hat{\mathbf{b}}_i\, d\mathbf{x}, \\
a &= \sum_j w_j^{\mathbf{r}} F_{\mathbf{r}}(\mathbf{r}_j) \sum_k w_k^{\mathbf{s}} F_{\mathbf{s}}(\mathbf{s}_k) \int_{\Xi(\mathbf{r})} \hat{a}\, d\mathbf{x}, \\
\mathbf{A} &= \begin{pmatrix} \mathbf{A}_{11} & \cdots & \mathbf{A}_{1n_m} \\ \vdots & \ddots & \vdots \\ \mathbf{A}_{n_m1} & \cdots & \mathbf{A}_{n_mn_m} \end{pmatrix}, \ \mathbf{b} = \begin{pmatrix} \mathbf{b}_1 \\ \vdots \\ \mathbf{b}_{n_m} \end{pmatrix} \text{ and } \mathbf{c} = \begin{pmatrix} \mathbf{C}_1 \\ \vdots \\ \mathbf{C}_{n_m} \end{pmatrix}.
\end{aligned} \tag{14}$$

With these notations, the objective function (9) is now expressed as a quadratic complex matrix form

$$J(\mathbf{c}) = \mathbf{c}^T\mathbf{A}\bar{\mathbf{c}} + \mathbf{c}^T\bar{\mathbf{b}} + \bar{\mathbf{c}}^T\mathbf{b} + a. \tag{15}$$

Eq. (15) is a complex-valued quadratic optimization program, which is not trivially solved. The imaginary part of quadratic function (15) is zero. Let us expand the real part of the objective function (15) as follows

$$\begin{aligned}
J(\mathbf{c}) = a &+ \sum_{i=1}^{n_m} \left(2\,\mathfrak{Re}\mathbf{C}_i^T\mathfrak{Re}\mathbf{b}_i + 2\,\mathfrak{Im}\mathbf{C}_i^T\mathfrak{Im}\mathbf{b}_i\right) \\
&+ \sum_{i=1}^{n_m}\sum_{j=1}^{n_m} \left(\mathfrak{Re}\mathbf{C}_i^T\mathfrak{Re}\mathbf{A}_{i,j}\mathfrak{Re}\mathbf{C}_j + \mathfrak{Im}\mathbf{C}_i^T\mathfrak{Re}\mathbf{A}_{i,j}\mathfrak{Im}\mathbf{C}_j\right. \\
&\left. - \mathfrak{Im}\mathbf{C}_i^T\mathfrak{Im}\mathbf{A}_{i,j}\mathfrak{Re}\mathbf{C}_j + \mathfrak{Re}\mathbf{C}_i^T\mathfrak{Im}\mathbf{A}_{i,j}\mathfrak{Im}\mathbf{C}_j\right).
\end{aligned} \tag{16}$$

By using notations in (14), this can be written in matrix form:

$$J(\mathbf{c}) = \begin{pmatrix} \mathfrak{Re}\mathbf{c} \\ \mathfrak{Im}\mathbf{c} \end{pmatrix}^T \begin{pmatrix} \mathfrak{Re}\mathbf{A} & \mathfrak{Im}\mathbf{A} \\ -\mathfrak{Im}\mathbf{A} & \mathfrak{Re}\mathbf{A} \end{pmatrix} \begin{pmatrix} \mathfrak{Re}\mathbf{c} \\ \mathfrak{Im}\mathbf{c} \end{pmatrix} \tag{17}$$

$$+2\begin{pmatrix} \mathfrak{Re}\mathbf{c} \\ \mathfrak{Im}\mathbf{c} \end{pmatrix}^T \begin{pmatrix} \mathfrak{Re}\mathbf{b} \\ \mathfrak{Im}\mathbf{b} \end{pmatrix} + a. \tag{18}$$

If we now further introduce notations

$$\tilde{\mathbf{A}} = 2\begin{pmatrix} \mathfrak{Re}\mathbf{A} & \mathfrak{Im}\mathbf{A} \\ -\mathfrak{Im}\mathbf{A} & \mathfrak{Re}\mathbf{A} \end{pmatrix}, \ \tilde{\mathbf{b}} = 2\begin{pmatrix} \mathfrak{Re}\mathbf{b} \\ \mathfrak{Im}\mathbf{b} \end{pmatrix} \text{ and } \tilde{\mathbf{c}} = \begin{pmatrix} \mathfrak{Re}\mathbf{c} \\ \mathfrak{Im}\mathbf{c} \end{pmatrix}, \tag{19}$$

we can express (15) as a real-valued quadratic optimization program

$$J(\mathbf{c}) = \frac{1}{2}\tilde{\mathbf{c}}^T\tilde{\mathbf{A}}\tilde{\mathbf{c}} + \tilde{\mathbf{c}}^T\tilde{\mathbf{b}} + a. \tag{20}$$

There are many efficient methods available problems of this form [9].

3.2 Optimality condition

If there are no constraints involved in the optimization problem, the linear mapping $\mathbf{C}$ is given by the optimality condition $\boldsymbol{\nabla}_{\mathbf{c}} J = \mathbf{0}$, which is equivalent with $\nabla_{\mathbf{c}}\mathfrak{Re}J$ as $\mathfrak{Im}J = 0$. This condition must be split into gradient with respect to real and imaginary parts of $\mathbf{c}$:

$$\begin{cases} \nabla_{\mathfrak{Re}\mathbf{c}} J = & 0, \text{ and} \\ \nabla_{\mathfrak{Im}\mathbf{c}} J = & 0. \end{cases} \tag{21}$$

To solve these conditions, the gradients of (21) are expanded by considering vector $\mathbf{c}$ in parts, i.e. the gradients with respect to real and imaginary parts of $\mathbf{C}_i$ are expanded as follows:

$$\begin{aligned}
\nabla_{\mathfrak{Re}\mathbf{C}_i} J(\mathbf{c}) &= 2\mathfrak{Re}\mathbf{b}_i \\
&\quad +2\mathfrak{Re}\mathbf{A}_{ii}\mathfrak{Re}\mathbf{C}_i - \left(\mathfrak{Im}\mathbf{C}_i^T\mathfrak{Im}\mathbf{A}_{ii}\right)^T + \mathfrak{Im}\mathbf{A}_{ii}\mathfrak{Im}\mathbf{C}_i \\
&\quad + \sum_{j\neq i}\Big(\mathfrak{Re}\mathbf{A}_{ij}\mathfrak{Re}\mathbf{C}_j + \mathfrak{Im}\mathbf{A}_{ij}\mathfrak{Im}\mathbf{C}_j \\
&\qquad\qquad + \left(\mathfrak{Re}\mathbf{C}_j^T\mathfrak{Re}\mathbf{A}_{j,i}\right)^T - \left(\mathfrak{Im}\mathbf{C}_j^T\mathfrak{Im}\mathbf{A}_{j,i}\right)^T\Big) \\
&= 2\mathfrak{Re}\mathbf{b}_i + 2\mathfrak{Re}\mathbf{A}_{ii}\mathfrak{Re}\mathbf{C}_i + 2\mathfrak{Im}\mathbf{A}_{ii}\mathfrak{Im}\mathbf{C}_i \\
&\quad + \sum_{j\neq i}\left(\mathfrak{Re}\mathbf{A}_{ij}\mathfrak{Re}\mathbf{C}_j + \mathfrak{Im}\mathbf{A}_{ij}\mathfrak{Im}\mathbf{C}_j + \mathfrak{Re}\mathbf{A}_{ij}\mathfrak{Re}\mathbf{C}_j + \mathfrak{Im}\mathbf{A}_{ij}\mathfrak{Im}\mathbf{C}_j\right) \\
&= 2\mathfrak{Re}\mathbf{b}_i + 2\mathfrak{Re}\mathbf{A}_{ii}\mathfrak{Re}\mathbf{C}_i + 2\mathfrak{Im}\mathbf{A}_{ii}\mathfrak{Im}\mathbf{C}_i \\
&\quad + \sum_{j\neq i}\left(2\mathfrak{Re}\mathbf{A}_{ij}\mathfrak{Re}\mathbf{C}_j + 2\mathfrak{Im}\mathbf{A}_{ij}\mathfrak{Im}\mathbf{C}_j\right) \\
&= 2\mathfrak{Re}\mathbf{b}_i + \sum_{j=1}^{n_m}\left(2\mathfrak{Re}\mathbf{A}_{ij}\mathfrak{Re}\mathbf{C}_j + 2\mathfrak{Im}\mathbf{A}_{ij}\mathfrak{Im}\mathbf{C}_j\right),
\end{aligned} \tag{22}$$

$$
\begin{aligned}
\nabla_{\mathfrak{Im}\mathbf{C}_i} J(\mathbf{c}) &= 2\mathfrak{Im}\mathbf{b}_i \\
&\quad +2\mathfrak{Re}\mathbf{A}_{ii}\mathfrak{Im}\mathbf{C}_i - \mathfrak{Im}\mathbf{A}_{ii}\mathfrak{Re}\mathbf{C}_i + \left(\mathfrak{Re}\mathbf{C}_i^T\mathfrak{Im}\mathbf{A}_{ii}\right)^T \\
&\quad + \sum_{j\neq i}\Big(\mathfrak{Re}\mathbf{A}_{ij}\mathfrak{Im}\mathbf{C}_j - \mathfrak{Im}\mathbf{A}_{ij}\mathfrak{Re}\mathbf{C}_j \\
&\qquad\qquad + \left(\mathfrak{Im}\mathbf{C}_j^T\mathfrak{Re}\mathbf{A}_{j,i}\right)^T + \left(\mathfrak{Re}\mathbf{C}_j^T\mathfrak{Im}\mathbf{A}_{j,i}\right)^T\Big) \\
&= 2\mathfrak{Im}\mathbf{b}_i + 2\mathfrak{Re}\mathbf{A}_{ii}\mathfrak{Im}\mathbf{C}_i - 2\mathfrak{Im}\mathbf{A}_{ii}\mathfrak{Re}\mathbf{C}_i \\
&\quad + \sum_{j\neq i}\left(\mathfrak{Re}\mathbf{A}_{ij}\mathfrak{Im}\mathbf{C}_j - \mathfrak{Im}\mathbf{A}_{ij}\mathfrak{Re}\mathbf{C}_j + \mathfrak{Re}\mathbf{A}_{ij}\mathfrak{Im}\mathbf{C}_j - \mathfrak{Im}\mathbf{A}_{ij}\mathfrak{Re}\mathbf{C}_j\right) \\
&= 2\mathfrak{Im}\mathbf{b}_i + 2\mathfrak{Re}\mathbf{A}_{ii}\mathfrak{Im}\mathbf{C}_i - 2\mathfrak{Im}\mathbf{A}_{ii}\mathfrak{Re}\mathbf{C}_i \\
&\quad + \sum_{j\neq i}\left(2\mathfrak{Re}\mathbf{A}_{ij}\mathfrak{Im}\mathbf{C}_j - 2\mathfrak{Im}\mathbf{A}_{ij}\mathfrak{Re}\mathbf{C}_j\right) \\
&= 2\mathfrak{Im}\mathbf{b}_i + \sum_{j=1}^{n_m}\left(2\mathfrak{Re}\mathbf{A}_{ij}\mathfrak{Im}\mathbf{C}_j - 2\mathfrak{Im}\mathbf{A}_{ij}\mathfrak{Re}\mathbf{C}_j\right). \qquad (23)
\end{aligned}
$$

Now, by using (22) and (23), we can write full gradient for (16) with respect to real and imaginary parts of $\mathbf{c}$ in matrix form:

$$
\begin{aligned}
\nabla_{\mathfrak{Re}\mathbf{c}} J(\mathbf{c}) &= \begin{pmatrix} \nabla_{\mathfrak{Re}\mathbf{C}_1} J(\mathbf{c}) \\ \vdots \\ \nabla_{\mathfrak{Re}\mathbf{C}_{n_m}} J(\mathbf{c}) \end{pmatrix} \\
&= \begin{pmatrix} \mathfrak{Re}\mathbf{A}_{11} & \cdots & \mathfrak{Re}\mathbf{A}_{1n_m} & \mathfrak{Im}\mathbf{A}_{11} & \cdots & \mathfrak{Im}\mathbf{A}_{1n_m} \\ \vdots & \ddots & \vdots & \vdots & \ddots & \vdots \\ \mathfrak{Re}\mathbf{A}_{n_m1} & \cdots & \mathfrak{Re}\mathbf{A}_{n_mn_m} & \mathfrak{Im}\mathbf{A}_{n_m1} & \cdots & \mathfrak{Im}\mathbf{A}_{n_mn_m} \end{pmatrix} \begin{pmatrix} \mathfrak{Re}\mathbf{C}_1 \\ \vdots \\ \mathfrak{Re}\mathbf{C}_{2n_m} \end{pmatrix} \\
&\quad + \begin{pmatrix} \mathfrak{Re}\mathbf{b}_1 \\ \vdots \\ \mathfrak{Re}\mathbf{b}_{n_m} \end{pmatrix} \\
&= \begin{pmatrix} \mathfrak{Re}\mathbf{A} & \mathfrak{Im}\mathbf{A} \end{pmatrix} \begin{pmatrix} \mathfrak{Re}\mathbf{c} \end{pmatrix} + \begin{pmatrix} \mathfrak{Re}\mathbf{b} \end{pmatrix}, \qquad (24)
\end{aligned}
$$

$$
\begin{aligned}
\nabla_{\mathfrak{Im}\mathbf{c}} J(\mathbf{c}) &= \begin{pmatrix} \nabla_{\mathfrak{Im}\mathbf{C}_1} J(\mathbf{c}) \\ \vdots \\ \nabla_{\mathfrak{Im}\mathbf{C}_{n_m}} J(\mathbf{c}) \end{pmatrix} \\
&= \begin{pmatrix} -\mathfrak{Im}\mathbf{A}_{11} & \cdots & -\mathfrak{Im}\mathbf{A}_{1n_m} & \mathfrak{Re}\mathbf{A}_{11} & \cdots & \mathfrak{Re}\mathbf{A}_{1n_m} \\ \vdots & \ddots & \vdots & \vdots & \ddots & \vdots \\ -\mathfrak{Im}\mathbf{A}_{n_m1} & \cdots & -\mathfrak{Im}\mathbf{A}_{n_mn_m} & \mathfrak{Re}\mathbf{A}_{n_m1} & \cdots & \mathfrak{Re}\mathbf{A}_{n_mn_m} \end{pmatrix} \begin{pmatrix} \mathfrak{Im}\mathbf{C}_1 \\ \vdots \\ \mathfrak{Im}\mathbf{C}_{n_m} \end{pmatrix} \\
&\quad + \begin{pmatrix} \mathfrak{Im}\mathbf{b}_1 \\ \vdots \\ \mathfrak{Im}\mathbf{b}_{n_m} \end{pmatrix} \\
&= \begin{pmatrix} -\mathfrak{Im}\mathbf{A} & \mathfrak{Re}\mathbf{A} \end{pmatrix} \begin{pmatrix} \mathfrak{Im}\mathbf{c} \end{pmatrix} + \begin{pmatrix} \mathfrak{Im}\mathbf{b} \end{pmatrix}. \qquad (25)
\end{aligned}
$$

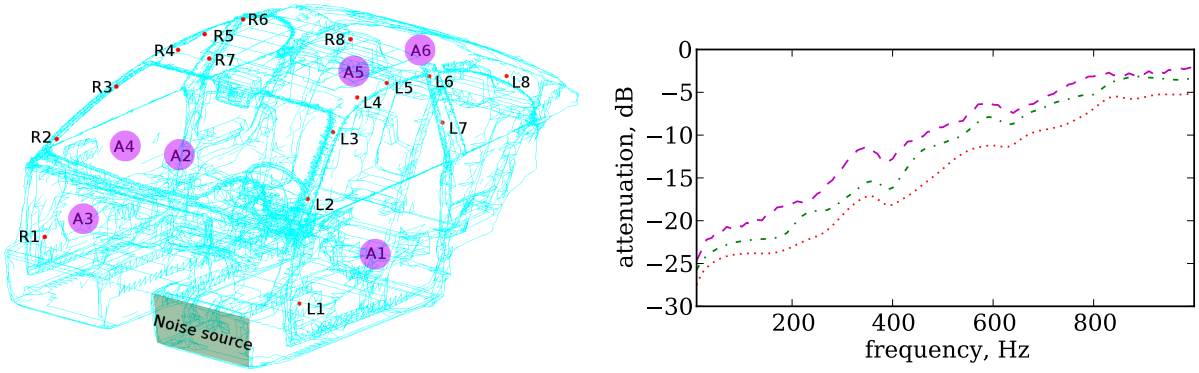

Figure 1: Left figure: noise and anti-noise sources (A1...A6) and measurement point locations (L1...L8, R1...R8). Right figure: ANC involves 2, 4 and 8 measurement points (magenta dashed line, green dot-dash line, and red dashed line, respectively).

We can now use (24) and (25) to express optimality condition (21) as a single linear system of equations:

$$\begin{pmatrix} \mathfrak{Re}\mathbf{A} & \mathfrak{Im}\mathbf{A} \\ -\mathfrak{Im}\mathbf{A} & \mathfrak{Re}\mathbf{A} \end{pmatrix} \begin{pmatrix} \mathfrak{Re}\mathbf{c} \\ \mathfrak{Im}\mathbf{c} \end{pmatrix} = -\begin{pmatrix} \mathfrak{Re}\mathbf{b} \\ \mathfrak{Im}\mathbf{b} \end{pmatrix}. \tag{26}$$

Furthermore, it can be now seen that (26) corresponds to complex-valued system of linear equations $\bar{\mathbf{A}}\boldsymbol{c} = -\mathbf{b}$, which has the solution

$$\mathbf{c} = -\bar{\mathbf{A}}^{-1}\mathbf{b}. \tag{27}$$

4 NUMERICAL DEMONSTRATION

The proposed local noise control method is demonstrated as by a numerical study of local active noise control in BMW 330i car interior (see Fig. 1). We will assume that there is a driver in otherwise empty car, so the computation domain $\Omega(\mathbf{r})$ for acoustical sound pressure field is defined by the cabin interior excluding the driver. Objective is to minimize noise in driver's ears, thus the silent region V_C (c.f. (7)) is defined as a set of two points, $V_C(\mathbf{r}) = \{\mathbf{x}^{e_l}(\mathbf{r}), \mathbf{x}^{e_r}(\mathbf{r})\} \subset \Omega(\mathbf{r})$, where $\mathbf{x}^{e_l}(\mathbf{r})$ and $\mathbf{x}^{e_r}(\mathbf{r})$ are the co-ordinates of the driver's left and right ear, respectively.

The stochasticity of the domain is here caused by the random movements of the driver. As in [3], the domain stochasticity variable $\mathbf{r} = (r_1, r_2, r_3)^T$ consists of three parameters: r_1 is driver's sideways bending angle, r_2 is forward bending angle, and r_3 is head rotation angle to left/right (see Fig. 1); all angles are in degrees. The distribution function $F_{\mathbf{r}}$ is given by a piecewise trilinear function that is defined by nodal values of a sampling over probability space, and elsewhere by trilinear interpolation. We will use sampling $\mathbf{r} \in \mathbf{R} = R_1 \times R_2 \times R_3$, where

$$\begin{aligned} R_1 &= \{-30.0, -20.0, -10.0, 0.0, 10.0, 20.0, 30.0\}, \\ R_2 &= \{-10.0, -5.0, 0.0, 5.0, 10.0, 15.0, 20.0\}, \text{ and} \\ R_3 &= \{-75.0, -50.0, -25.0, 0.0, 25.0, 50.0, 75.0\}. \end{aligned} \tag{28}$$

The corresponding expected value integral in (8) is approximated by the three-dimensional trapezoidal quadrature rule.

The noise source is modeled as a vibrating quadrangular surface behind the leg room, which approximates the real noise source (see Fig. 1). The amplitude f (see (2)) of the noise source is given by a bilinear function defined by the corner values $f(x_i, y_i) = s_i$, $i = 1 \ldots 4$, where s_i denotes amplitude coefficient for ith corner of the source quadrangle, located in (x_i, y_i). The noise source stochasticity variable is thus defined as $\mathbf{s} = (s_1, s_2, s_3, s_4)^T$. The distribution functions $F_{\mathbf{s}}$ is given by a piecewise quadrilinear function that is defined by the nodal values of a sampling over probability space, and elsewhere by quadrilinear interpolation. We will use sampling $\mathbf{s} \in \mathbf{S} = S_1 \times S_2 \times S_3 \times S_4$, where $S_1 = S_2 = S_3 = S_4 = \{0.5,\ 0.75,\ 1.0,\ 1.25,\ 1.5\}$. The corresponding expected value integral in (8) is approximated by the four-dimensional generalization of the trapezoidal quadrature rule.

The Helmholtz equation (1) was solved with the finite element method. Meshes consisting of linear tetrahedra and triangles were generated with Ansys ICEM CFD meshing software; the meshes were generated so that there are at least 10 nodes per wavelength at $f = 1000\,\text{Hz}$. Measurement point locations are presented in Fig. 1 and they are labeled as follows: L1...L8 for left side measurement points and R1...R8 for right side measurement points. The absorbency coefficients η in (2) were set approximately for each material. The study was performed in the frequency range 10–1000 Hz with 10 Hz steps.

In Fig. 1, the solution obtained by the method is plotted when 2, 4 and 8 measurement points are used in optimizing ANC performance. The optimality condition (27) is used to optimize the coefficient matrix $\mathbf{C}$ for each frequency, six anti-noise actuators are being used (see Fig. 1). It is seen that increasing the number of measurement points enhances the noise control. Especially good results (over 20 dB attenuation) are obtained with lower frequencies.

5 CONCLUSIONS

The least-squares quadratic optimization formulation for an advanced local noise control method based on stochastic finite element domains was given. The method presented in this paper intelligently uses information obtained by numerical acoustical modeling, which allows to obtain substantially better noise control than with traditional local ANC methods, with respect to both attenuation level and it's focusing on right place. The stochasticity of the noise source made the model significantly more realistic and linear mapping makes it possible to use precise time-dependent phase and amplitude information such that the noise control is adapted to prevailing conditions. The method was demonstrated by a local noise control in a car cabin and good results (over 20 dB attenuation) were obtained, especially with low frequencies.

ACKNOWLEDGMENTS

The research was funded by Academy of Finland, grants #250979 and #252549.

REFERENCES

[1] T. Airaksinen and T. Aittokoski. Multi-objective actuator placement optimization for local sound control evaluated in a stochastic domain. In S. Repin, T. Tiihonen, and T. Tuovinen, editors, *Numerical methods for differential equations, optimization, and technological problems*. Springer, 2012. accepted.

[2] Tuomas Airaksinen, Erkki Heikkola, Anssi Pennanen, and Jari Toivanen. An algebraic multigrid based shifted-Laplacian preconditioner for the Helmholtz equation. *J. Comput. Phys.*, 226(1):1196–1210, 2007.

[3] Tuomas Airaksinen, Erkki Heikkola, and Jari Toivanen. Local control of sound in stochastic domains based on finite element models. *J. Comput. Acoust.*, 19(2):205–219, Jun 2011.

[4] Tuomas Airaksinen, Anssi Pennanen, and Jari Toivanen. A damping preconditioner for time-harmonic wave equations in fluid and elastic material. *J. Comput. Phys.*, 228(5):1466–1479, 2009.

[5] Alfredo Bermúdez, Pablo Gamallo, and Rodolfo Rodríguez. Finite element methods in local active control of sound. *SIAM J. Control Optim.*, 43(2):437–465, 2004.

[6] A. Brancati and M. H. Aliabadi. Boundary element simulations for local active noise control using an extended volume. *Eng. anal. bound. elem.*, 36(2):190–202, 2012.

[7] M. Misol, S. Algermissen, and H. P. Monner. Experimental investigation of different active noise control concepts applied to a passenger car equipped with an active windshield. *J. Sound Vib.*, 331(10):2209–2219, 2012.

[8] P. A. Nelson and S. J. Elliot. *Active control of sound*. Academic Press, London, 1999.

[9] J. Nocedal and S. J. Wright. *Numerical optimization*. Series in Operations Research and Financial Engineering. Springer, New York, second ed. edition, 2006.

[10] C. G. Provatidis, S. T. Mouzakitus, and G. N. Charalampoloulos. Simulation of active noise control in enclosures using direct sound field prediction. *J. Comput. Acoustics*, 17(1):83–107, 2009.

[11] J. M. Sousa, C. A. Silva, and J. M. G. Sá da Costa. Fuzzy active noise modeling and control. *Int. J. Approx. Reason.*, 33(1):51–70, 2003.

[12] D. A. Stanef, C. H. Hansen, and R. C. Morgans. Active control analysis of mining vehicle cabin noise using finite element modelling. *J. Sound Vib.*, 277(1-2):277–297, 2004.

[13] L. L. Thompson. A review of finite-element methods for time-harmonic acoustics. *J. Acoust. Soc. Am.*, 119(3):1315–1330, March 2006.

[14] Wen-Kung Tseng. Local active noise control using a novel method of designing quiet zones. *Control Eng. Pract.*, 19(12):1450–1458, 2011.